Nanostructured SnSb/Carbon Nanotube Composites Synthesized by Reductive Precipitation for Lithium-Ion Batteries

Min-Sik Park,[†] Scott A. Needham,[†] Guo-Xiu Wang,[†,‡] Yong-Mook Kang,*[,§] Jin-Soo Park,[†] Shi-Xue Dou,[†] and Hua-Kun Liu[†]

Institute for Superconducting and Electronic Materials and ARC Centre of Excellence for Electromaterials Science and School of Mechanical, Materials and Mechatronic Engineering, University of Wollongong, NSW 2522, Australia, and Energy Lab, Samsung SDI Company, 428-5 Gongse-ri, Giheung-eup, Yongin-si, Gyeonggi-do, Republic of Korea

Received January 19, 2007. Revised Manuscript Received March 15, 2007

Nanosized particles of SnSb alloy were coated on the surface of multiwalled carbon nanotubes (CNTs) by reductive precipitation of metal chloride salts within a CNT suspension. The SnSb−CNT nanocomposite showed a high reversible capacity of 480 mAh g^{-1} and stable cyclic retention until the 50th cycle. The improvement of reversible capacity and cyclic performance of the SnSb−CNT composite is attributed to the nanoscale dimension of the SnSb alloy particles (<50 nm) and the structural advantages of CNTs as a framework material. The CNTs could be pinning the SnSb alloy particles on their surfaces so as to hinder the agglomeration of SnSb particles, while maintaining electronic conduction as well as accommodating drastic volume variation during electrochemical reactions.

Introduction

In the lithium-ion battery field, much attention has been paid to nanostructured materials such as nanowires,[1] nanotubes,[2] and nanocomposites[3] because of the significant advantages of their kinetics during the lithiation and delithiation processes. In fact, the nanostructured electrode materials have shown enhanced Li^+ storage and electronic conduction, which may accelerate the development of high-energy-density lithium-ion batteries. In this respect, many nanosized alloys have been investigated that are capable of capacities far in excess of that of commercial graphite (for LiC_6, 372 mAh g^{-1}).[4−6]

Nanosized SnSb intermetallic alloys are a promising group of high-capacity alloys that offer three advantageous design features: (1) both Sn ($Li_{4.4}Sn$, 990 mAh g^{-1}) and Sb (Li_3Sb, 660 mAh g^{-1}) elements contribute to the specific capacity of Li^+, but at different stages in the electrochemical discharge process;[7,8] (2) the large volume variations of the cycled alloys due to the insertion/extraction of Li^+ can be effectively accommodated by a highly dispersed ductile Sn phase;[9] and (3) nanosized powders can lead to the enhanced kinetic properties during electrochemical reactions.[10,11] Despite these desirable features, the practical capacity and cycling performance of these alloys are often limited by the agglomeration in nanoscale form. This can reduce the alloy's ability to restrain volume variations and lead to cracking and crumbling of the electrode.[5,10] Recently, the demand for stable cyclic performance of nanosized SnSb alloys have highly stimulated the research for nanocomposites with carbonaceous materials such as graphite,[9] MCMB,[10] and amorphous carbon.[12] However, the agglomeration of nanosized alloys is still considered as the predominant barrier to the practical application of these nanoscale alloys.

On the other hand, carbon nanotubes (CNTs) have also been extensively investigated as a nanoscale framework material for electronic devices because of their extraordinary thermal and mechanical stability and high electronic conductivity.[13−15] Compared to other carbonaceous electrodes, CNT electrodes can react at a lower potential and accommodate more Li^+ because of their wider *d*-spacing (CNT, 0.34 nm; graphite, 0.33 nm) and larger surface to

* Corresponding author. Tel: 82-16-257-9051. Fax: 82-31-210-7555. E-mail: dake@kaist.ac.kr.
† Institute for Superconducting and Electronic Materials and ARC Centre of Excellence for Electromaterials Science, University of Wollongong.
‡ School of Mechanical, Materials and Mechatronic Engineering, University of Wollongong.
§ Samsung SDI.

(1) Li, W. Y.; Xu, L. N.; Chen, J. *Adv. Funct. Mater.* **2005**, *15*, 851.
(2) Li, N.; Martin, C. R.; Scrosati, B. *Electrochem. Solid-State Lett.* **2000**, *3*, 316.
(3) Park, M. S.; Wang, G. X.; Kang, Y. M.; Kim, S. Y.; Liu, H. K.; Dou, S. X. *Electrochem. Commun.* **2007**, *9*, 71.
(4) Yang, J.; Winter, M.; Besenhard, J. O. *Solid State Ionics* **1996**, *90*, 281.
(5) Li, H.; Shi, L.; Wang, Q.; Chen, L.; Huang, X. *Solid State Ionics* **2002**, *148*, 247.
(6) Rönnebro, E.; Yin, J.; Kitano, A.; Wada, M.; Tanase, S.; Sakai, T. *J. Electrochem. Soc.* **2005**, *152*, A152.
(7) Huggins, R. A. *J. Power Sources* **1999**, *81*−*82*, 13.
(8) Winter, M.; Besenhard, J. O.; Spahr, M.; Novak, P. *Adv. Mater.* **1998**, *10*, 725.
(9) Needham, S. A.; Wang, G. X.; Liu, H. K. *J. Alloys Compd.* **2005**, *400*, 234.
(10) Shi, L.; Li, H.; Wang, Z.; Huang, X.; Chen, L. *J. Mater. Chem.* **2001**, *11*, 1502.
(11) Besenhard, J. O.; Wachtler, M.; Winter, M.; Andreaus, R.; Rom, I.; Sitte, W. *J. Power Sources* **1999**, *81*−*82*, 268.
(12) Li, H.; Wang, Q.; Shi, L.; Chen, L.; Huang, X. *Chem. Mater.* 2002, **14**, 103.
(13) Frackowiak, E.; Gautier, S.; Gaucher, H.; Bonnamy, S.; Beguin, F. *Carbon* **1999**, *37*, 61.
(14) Gao, B.; Kleinhammes, A.; Tang, X. P.; Bower, C.; Fleming, L.; Wu, Y.; Zhou, O. *Chem. Phys. Lett.* **2000**, *307*, 153.
(15) Wu, G. T.; Wang, C. S.; Zhang, X. B.; Yang, F. S.; Qi, Z. F.; He, P. M.; Li, W. Z. *J. Electrochem. Soc.* **1999**, *146*, 1696.

10.1021/cm0701761 CCC: $37.00
Published on Web 04/17/2007

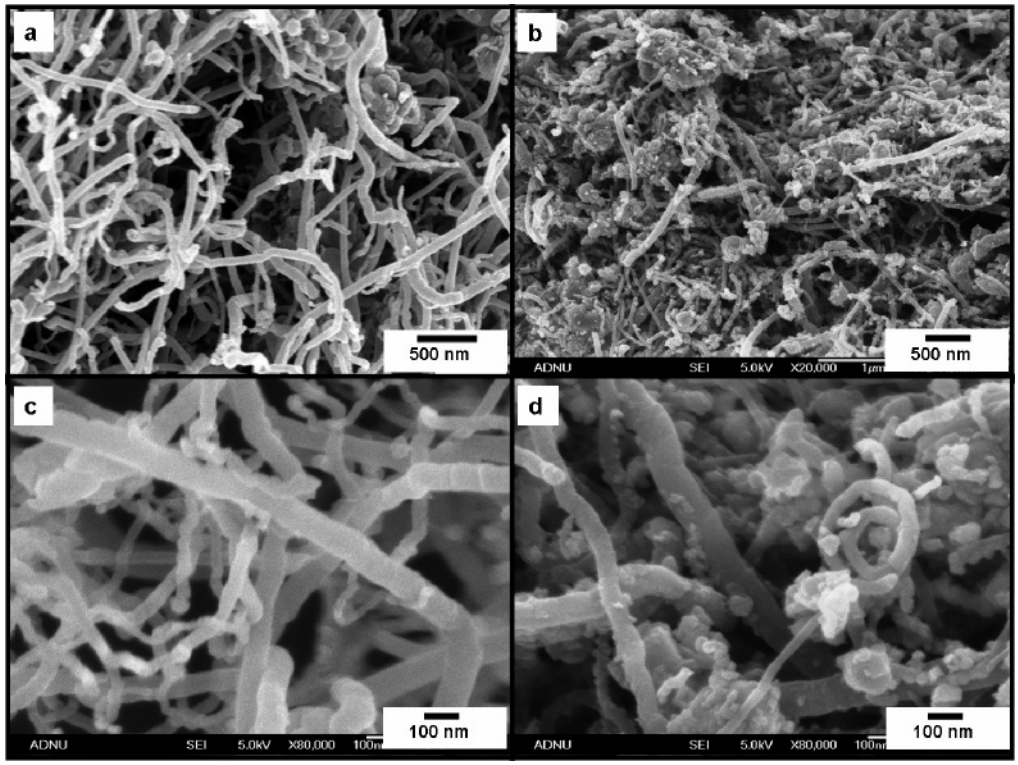

Figure 1. Microstructure of SnSb−CNT nanocomposite and normal CNTs: (a, c) field-emission SEM images of normal multiwalled CNTs; (b, d) field-emission SEM images of SnSb−CNT nanocomposite prepared by reductive precipitation of metal salts at different magnification levels.

volume ratio.[16] It can be a promising candidate for reducing electrochemical degradations induced by the agglomeration of nanosized SnSb alloys.[17]

In this study, the nanosized SnSb alloy particles were simply coated on the surface of CNTs by reductive precipitation of metal chloride salts within a CNT suspension. By using this method, we avoided the drastic volume variation and agglomeration of SnSb alloys, which resulted in a significant improvement in electrochemical performance of the electrode. The structural and electrochemical properties of the SnSb−CNT nanocomposite are presented and characterized with the aim of application for lithium-ion batteries.

SEM observation shows a general view of SnSb−CNT nanocomposite compared with normal CNTs. Images a and c of Figure 1show randomly aligned normal CNTs with an outer diameter of approximately 50−100 nm and a length of 200−300 μm at different magnification levels. The morphology of the SnSb−CNT nanocomposite was also observed in order to confirm the morphological changes after the reductive precipitation process as shown in images b and d of Figure 1, which clearly show the uniform distribution of SnSb nanoparticles on the surface of the CNTs.

The weight percent of Sn, Sb, and CNTs was estimated to be 24.91, 22.69, and 52.40 wt %, respectively, and there was no evidence of Cl^- in the obtained nanocomposites according to an elemental analysis using selected area energy-dispersive X-ray spectrometry (EDS). This result reveals that the composition of SnSb nanoparticles in the composites can be assumed to be $Sn_{1.05}$ $Sb_{0.95}$ phase, which is in excellent

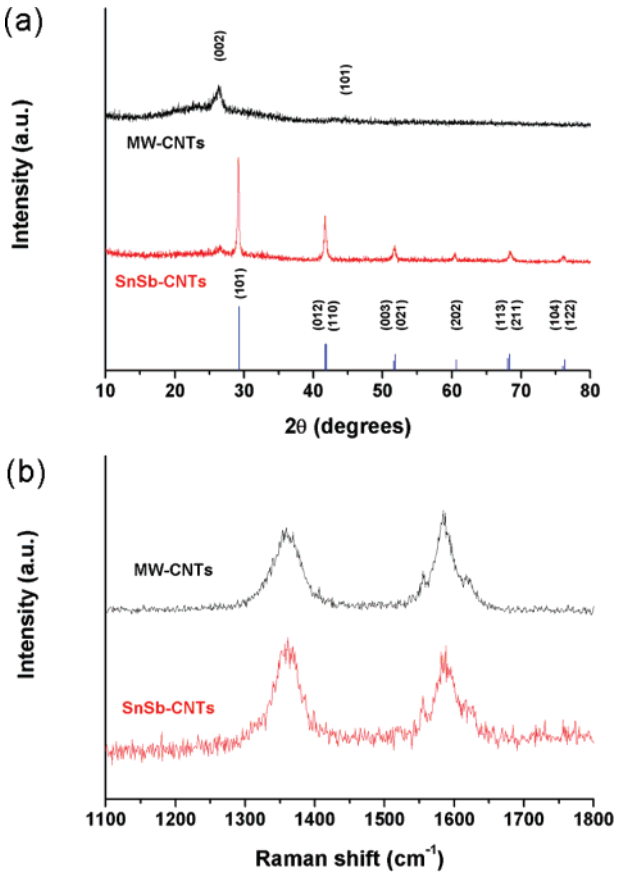

Figure 2. (a) X-ray diffraction patterns and (b) room-temperature Raman spectrum of SnSb−CNT nanocomposite compared to the normal multiwalled CNTs.

accordance with the X-ray diffraction patterns in Figure 2a. All reflections of the SnSb−CNT nanocomposite correspond to the β-SnSb phase (JCPDS #33−0118), which belongs

(16) Chen, W. X.; Lee, J. Y.; Liu, Z. *Electrochem. Commun.* **2002**, *4*, 260.
(17) Guo, Z. P.; Zhao, Z. W.; Liu, H. K.; Dou, S. X. *Carbon* **2005**, *43*, 1392.

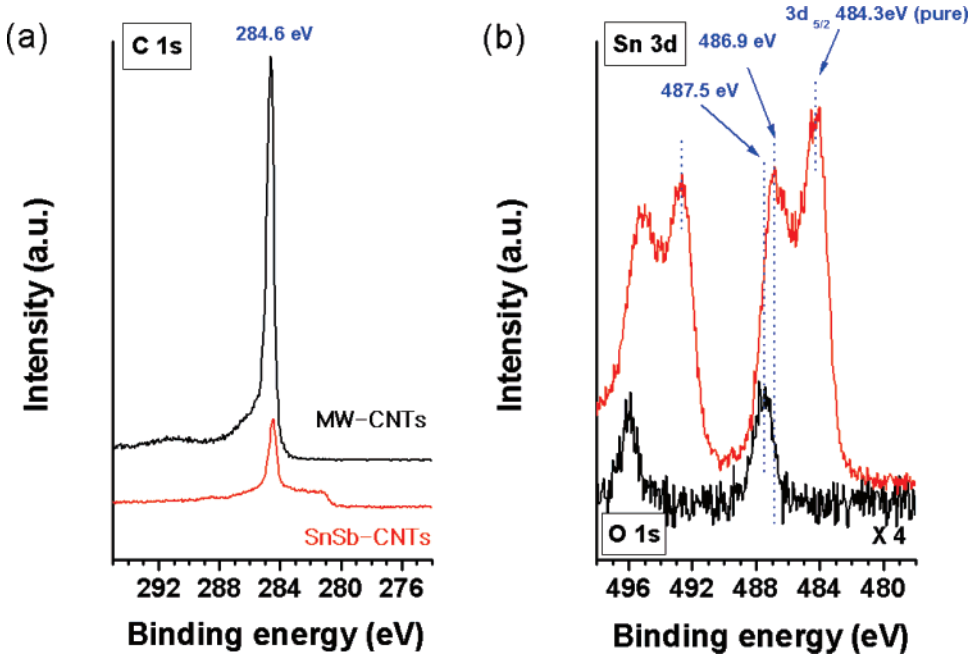

Figure 3. (a) XPS C 1s narrow scan spectra for multiwalled CNTs (black line) and SnSb−CNT nanocomposite (red line); (b) XPS Sn 3d narrow scan spectra for SnSb−CNT nanocomposite (for a comparative purpose, XPS O 1s spectra for CNTs were displayed.)

to the space group R-$_3m$ (166). The lattice parameters of coated SnSb alloy are $a = b = 4.3251$ Å and $c = 5.3376$ Å in a rhombohedral structure. There was no evidence of any kind of Sn-related or other phases apart from the (002) and (101) peaks of CNTs.

The room-temperature Raman spectra show a difference in the crystallinity of CNTs before and after the reductive precipitation process. It is well-known that CNTs possess two peaks at 1354 cm^{-1} (*D* band) and 1581 cm^{-1} (*G* band). After the reductive precipitation, the I_G/I_D ratio of the CNTs has been changed from 1.22 to 0.87, as shown in Figure 2b. The decrease in the ratio indicates that the atomic ordering or crystallinity of the CNTs was reduced, and suggests that the precipitation of polycrystalline SnSb involved the formation of some chemical bonds with the CNTs surfaces, rather than only physical adsorption.[18,19]

The destructive nature of precipitation could be also confirmed by X-ray photoelectron spectroscopy (XPS) analysis. Figure 3a shows the C 1s spectra for CNT and SnSb−CNT nanocomposite. The C 1s binding energy of the CNT used for the SnSb−CNT nanocomposite was about 284.6 eV, which corresponds to the typical binding energy of C−C bonding. On the other hand, the C 1s spectrum indicated that the binding energy was convoluted from various types of bonding, such as C−C bonding and Sn−C bonding (283.4 eV). Because the electronegativity of Sn is 1.8 and that of carbon is 2.5, the carbon atom localizes the electrons around Sn−C bonds. Therefore, the C 1s binding energy for Sn−C bonding tends to show a negative chemical shift. The existence of Sn−C bonding was clearly proven by the bonding states of Sn atoms as determined from the Sn $3d_{5/2}$ spectrum. As shown in Figure 3b, the Sn $3d_{5/2}$ spectrum is composed of two main peaks located at 484.3 and 486.9 eV. Because the Sn $3d_{5/2}$ binding energies for Sn−Sn bonding and Sn−C bonding have been reported to be about 484.6 and 486.3 eV, respectively, we could conclude that at the interface between SnSb and CNT, Sn−C bonding was evolved from the destruction of C−C bonding.[20,21] This chemical bonding would change the surface topography of the materials and produce additional highly reactive defects sites such as dangling bonds and pores. It was also found that the surface area of the CNTs increased from 55.12 m^2 g^{-1} to 61.36 m^2 g^{-1} because of these defects and the presence of the SnSb nanoparticles on the surface of CNTs.

Figure 4 shows typical TEM images of the SnSb−CNT nanocomposite at various magnification levels. As shown in Figure 4a, the selected area diffraction (SAD) pattern (inset) indicates that the composite consists of CNTs and polycrystalline SnSb nanoparticles. From the figure, it can be observed that the SnSb alloy particles with a size of 30−50 nm on average are well-coated onto the CNTs. In the higher-resolution image of Figure 4c, it is made clear that the average grain size of the SnSb alloys is less than 10 nm with a *d*-spacing of 0.53 nm, thus confirming their polycrystalline nature.

It is well-known that if the particle size of SnSb alloy is less than 100 nm, the particles would be agglomerated because of the overwhelming driving force to reduce their surface energy.[5,10] However, in our samples, the agglomeration of SnSb alloys was adequately prevented by the formation of a SnSb−CNT composite. It is surmised that the additional induced defects like dangling bonds acted as nucleation sites on which the alloy particles were precipitated. In this way, the Sn^{2+} and Sb^{3+} ions would substitute for C atoms at an atomic level to act as seeds at the initial stage

(18) Endo, M.; Nishimura, K.; Kim, Y. A.; Hakamada, K.; Matushita, T.; Dresselhaus, M. S.; Dresselhaus, G. *J. Mater. Res.* **1999**, *14*, 4474.
(19) Tan, P. H.; Zhang, S. L.; Yue, K. T.; Huang, F. M.; Shi, Z. J.; Zhou, X. H.; Gu, Z. N. *J. Raman Spectrosc.* **1997**, *28*, 369.
(20) Wagner, C. D.; Gale, L. H.; Raymond, R. H. *Anal. Chem.* **1979**, *51*, 466.
(21) Inoue, Y.; Takai, Proc, O. *Symp. Plasma Sci. Mater.* **1996**, *9*, 39.

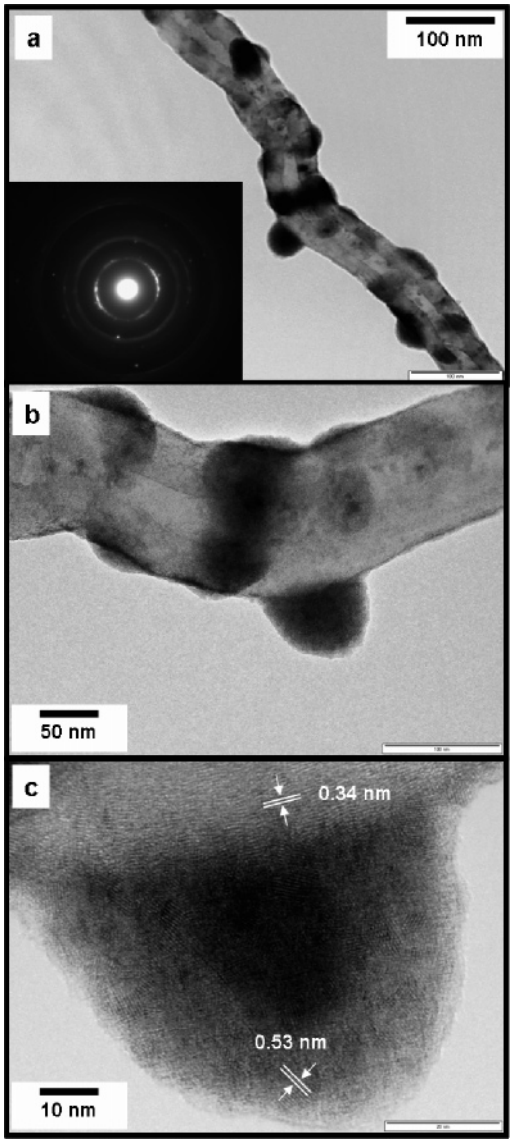

Figure 4. (a) TEM image and selected area diffraction (SAD) pattern (inset) of SnSb−CNT nanocomposite, (b) TEM image of an individual SnSb−CNT nanocomposite at a high magnification level, and (C) HRTEM image of SnSb alloy nanoparticle coated on the surface of a CNT.

of the precipitation. Therefore, we can suggest that the reductive precipitation method is appropriate to pin SnSb nanoparticles onto CNTs, preventing the agglomeration of the SnSb nanoparticles.

The anodic performance of the SnSb−CNT nanocomposite was tested in the potential range from 0.05 to 1.5 V (vs Li/Li^+). For comparative purpose, normal CNTs were also examined under the same conditions. As plotted in Figure 5a, the SnSb−CNT nanocomposite showed an initial discharge capacity of 1408 mAh g^{-1} and an irreversible capacity of 728 mAh g^{-1} in the galvanostatic voltage profile for the first cycle. It should be noted that the SnSb−CNT nanocomposite showed an initial coulombic efficiency of approximately 48.30%, which was notably higher than that of the normal CNTs, 34.75%. The improvement of the initial coulombic efficiency can be attributed to the SnSb phase, which would react with Li^+ during the electrochemical reaction. The charge−discharge reactions of the SnSb−CNT nanocomposite electrodes were reversible over cycles without any significant capacity fading induced by agglomerations

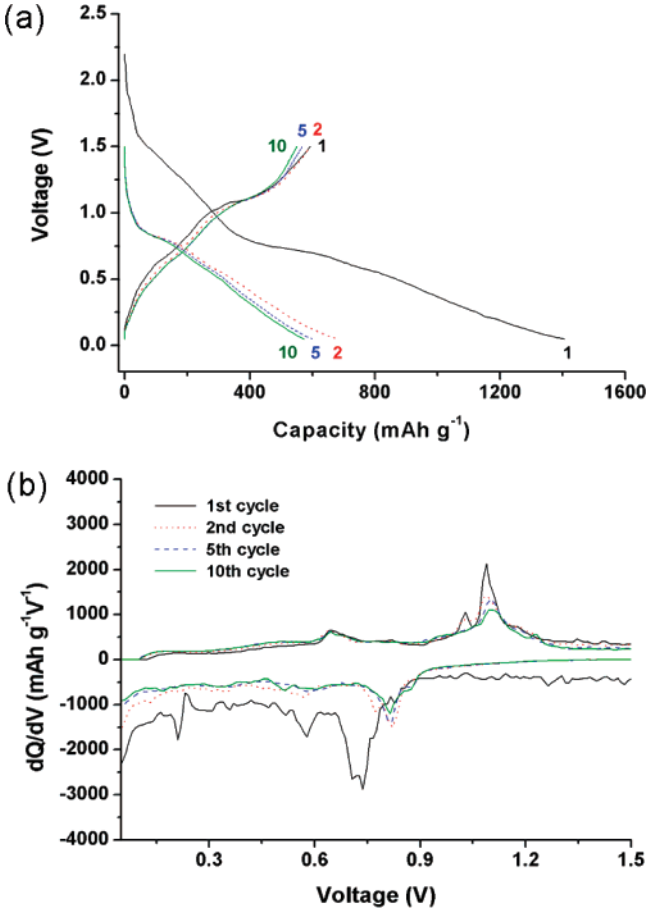

Figure 5. Anodic performance of the SnSb−CNT nanocomposite: (a) galvanostatic voltage profiles between 0.05 and 1.5 V; (b) differential charge−discharge versus potential plots at the first, second, fifth, and tenth cycle between 0.05 and 1.5 V for the SnSb−CNT nanocomposite.

in the nanosized SnSb alloy.[5] This was because the network structure of CNTs is fit not only for pinning SnSb alloy nanoparticles, but also for maintaining the electronic conduction around the active phases, in spite of their enormous volume variation during Li^+ insertion or extraction. However, there was a clear tradeoff between the initial coulombic efficiency and cyclic retention because the adoption of CNT as the supporting material for SnSb involved the augmented initial irreversible capacity induced by trapping Li^+ in its inner holes or defects.

To identify all of the electrochemical reactions, the differential charge−discharge capacity vs voltage profiles of SnSb/CNT nanocomposite are presented in Figure 5b. The first differential discharge profile shows a major reduction peak around 0.75 V derived from Li_3Sb formation when Sb phase reacts with Li^+ according to eq 1 below, and numerous small peaks from 1.5 to 0.75 V, which were evolved by electrolyte decomposition or solid electrolyte interphase (SEI) film formation. The apparent peaks at 0.2 and 0.55 V seem to be formed by an irreversible reaction between Li^+ and defects or buckled layers of CNTs. These reactions definitely involve an irreversible process, because the peaks disappeared in subsequent cycles. The reversible alloying and dealloying reaction of SnSb due to reaction with Li^+ is described in eq 2 below.[6] Graphically, this process is clearly represented from the second cycle by the reduction peak at 0.85 V and the oxidation peak at 1.1 V. The other pairs of

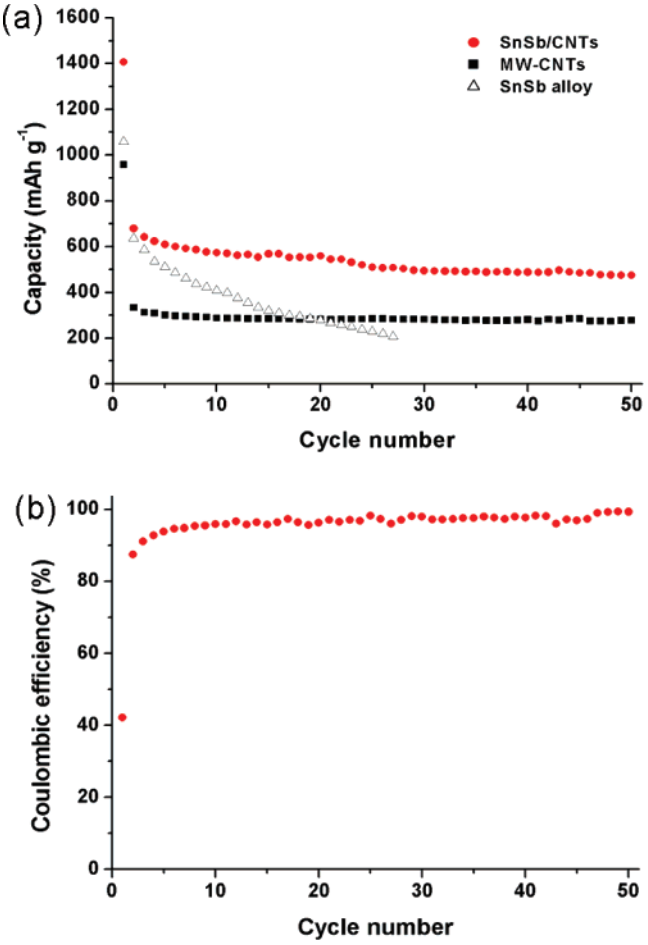

Figure 6. Anodic performance of the SnSb−CNT nanocomposite: (a) cyclic performance of SnSb−CNT nanocomposite and normal CNTs up to the 50th cycle at the same current density, 100 mA g^{-1}; and (b) the coulombic efficiency of SnSb−CNT nanocomposite electrode up to the 50th cycle.

reduction peaks between 0.25 and 0.7 V during discharging and oxidation peaks between 0.4 and 0.8 V during charging are related to the formation of various Li_xSn alloys as described in the eq 3.[3] Both reduction and oxidation peaks below 0.2 V are correlated with the intercalation and deintercalation of Li^+ into the CNTs.

$$SnSb + 3Li^+ + 3e^- \rightarrow Sn + Li_3Sb \quad (1)$$

$$SnSb + Li \leftrightarrow Li_{2x+1}Sn_{1-x}Sb + Sn \quad (2)$$

$$Sn + yLi^+ + ye^- \leftrightarrow Li_ySn\ (0 \le y \le 4.4) \quad (3)$$

The SnSb−CNT nanocomposite exhibits good cyclic performance, a high reversible specific capacity (>480 mAh g^{-1}), and high coulombic efficiency (>95%) up to the 50th cycle, as shown in panels a and b of Figure 6. This indicates that the nanosized SnSb alloy contributed to the increases in Li^+ storage, whereas randomly distributed CNTs contributed to maintaining the electronic conduction around the SnSb alloy particles, as well as accommodating the volume variation that was mainly induced by the reaction between Li^+ and SnSb. From the viewpoint of electrochemical properties, CNT is apparently superior to other carbonaceous materials such as graphite,[9] MCMB,[10] and amorphous carbon.[12] Because the structure of CNT is more adaptable to the homogeneous dispersion of SnSb nanoparticles than other carbonaceous materials, loading a large amount of SnSb particles into the composite can achieve a higher capacity. There is evidence to believe that CNTs more effectively prevent the agglomeration of nanosized SnSb particles and therefore retain the enhanced electrical properties of the SnSb alloy in nanoscale form. On the basis of this result and discussion, it could be concluded that the reversible capacity loss or electrical disconnection induced by the agglomeration of nanosized SnSb alloy could be effectively reduced in the SnSb−CNT nanocomposite prepared by the reductive precipitation process.

In summary, we have fabricated SnSb−CNT nanocomposite by means of reductive precipitation of metal chloride salts. The CNTs were a sort of framework used to pin nanosized SnSb particles on the surface and, as a result, hinder the agglomeration of SnSb nanoparticles. Several structural analyses clearly showed that SnSb particles were homogeneously precipitated on CNT with the help of Sn−C bonding between SnSb and CNT. SnSb−CNT nanocomposite showed an enhanced reversible capacity (>480 mAh g^{-1}) and stable cyclic retention because the drastic volume variation due to the agglomeration of SnSb alloy particles was effectively reduced during the electrochemical reaction. It could be clearly seen that CNTs were suitable for pinning nanosized SnSb particles and preventing their agglomeration, as well as maintaining the electrical connection around the SbSb particles. However, there was a unique drawback, that the increased initial irreversible capacity caused by the trapped Li^+ in the inner holes or defects of CNT. Finally, careful attention to the design and fabrication of these types of complex nanocomposites may lead to their full potential being exploited in commercial lithium ion batteries.

Acknowledgment. Financial support provided by the Australian Research Council (ARC) through an ARC Centre of Excellence project (CE0561616) and an ARC Discovery project (DP0559891) are gratefully acknowledged. The authors thank Dr. T. Silver at the University of Wollongong (Australia) and Dr. H.S. Kim at the Universty of Pennsylvania for their contributions.

Supporting Information Available: Experimental details and Figures 7 and 8. This material is available free of charge via the Internet at http://pubs.acs.org.

CM0701761